Optics Communications 569 (2024) 130847

Contents lists available at ScienceDirect

Optics Communications

journal homepage: www.elsevier.com/locate/optcom

Experimental performance of a two-receivers and two-transmitters array X-ray communication system

Hao Chi [a], Yunpeng Liu [a,b,*], Junxu Mu [a], Feixu Xiong [a], Xiaobin Tang [a,b,**]

[a] Department of Nuclear Science and Technology, Nanjing University of Aeronautics and Astronautics, Nanjing, 210016, China
[b] Key Laboratory of Nuclear Technology Application and Radiation Protection in Astronautics, Ministry of Industry and Information Technology, Nanjing, 210016, China

ARTICLE INFO

Keywords:
Array X-ray communication
Plastic scintillator
Spatial correlation coefficients
Bit error rate

ABSTRACT

In this work, we constructed a two-transmitter, two-receiver array based on grid-controlled modulated X-ray tubes and plastic-scintillator-coupled SiPM detectors to improve the communication rate of X-ray communication (XCOM) systems. The effects of various working parameters, and array dimensions on the bit-error-rate of the system were investigated. We derived the relationship between array dimensions and spatial correlation coefficient theoretically, and pointed out that a higher spatial correlation coefficient is the main reason affecting system performance experimentally. The array communication system achieves a communication data rate of 3.6 Mbps under a 12.5 cm laboratory atmospheric channel with a moderate spatial correlation coefficient of 0.5. The array XCOM system can effectively increase the data rate compared with previous work. This study can provide an experimental foundation and design reference for the establishment of a multiple-input, multiple-output array XCOM system.

1. Introduction

X-ray communication (XCOM) is a wireless optical communication method that loads information on the characteristic parameters of X-rays for information transmission [1,2]. With the advantages of extremely high theoretical bandwidth, a narrow diffraction limit, and good directionality and confidentiality, XCOM has high application prospects in reentry blackout communication, intersatellite communication, and aircraft navigation. Therefore, XCOM is known as "the next-generation aerospace communications technology [3,4]". A typical XCOM system consists of transmitters, such as the grid-controlled modulated X-ray tube (GMXT), light-controlled modulated X-ray tube (LMXT), and field emission X-ray tube (FEXT) [5,6], receivers, such as silicon drift detectors (SDD) [7], the scintillator lutetium–yttrium oxyorthosilicate (LYSO) couple with silicon photomultiplier (SiPM) detectors [8], and avalanche photodiode detectors (APD) [9], and focusing-collimating devices [10]. Current research on X-ray communications is mainly based on the single-input, single-output (SISO) communication mode [11]. Li et al. achieved a data rate of 200 kbps in a wavelength division multiplexing system [12]. Timofeer et al. achieved a rate of 0.7 Mbps based on a photocathode X-ray source [13]. Xuan [6] and Liu [8] used different detectors to achieve data rates of 100 kbps with bit error rate (BER) at 9.21E-2, and 1.21 Mbps with BER at 1E-5, respectively. The bandwidth of current modulated X-ray tubes is typically several megahertz, and the fastest time resolution of X-ray detectors used in XCOM is approximately a few hundred nanoseconds [14,15]. These two parameters limit the further improvement in communication data rate of the SISO-XCOM system. The solution to further improve the XCOM system rate is to build a multiple-input, multiple-output (MIMO) X-ray communication system. A typical MIMO-XCOM system consists of multiple pulsed modulated X-ray sources, focusers/collimators, and multiple pulsed X-ray detectors, as shown in Fig. 1. MIMO uses the degrees of freedom in the spatial dimension to improve communication reliability [16–18]. The MIMO system divides the high-speed input signal into multiple low-speed signals. The low-speed signals are modulated and transmitted by different pulse transmission sources, and then received and demodulated by corresponding receivers to achieve high-speed signal transmission [16]. Since the fading process experienced by photons in different channel links is different, the MIMO system can also effectively combat link fading by selecting an appropriate signal combining method. However, since the photon beam reaching the receiver drifts and broadens, and

* Corresponding author. Department of Nuclear Science and Technology, Nanjing University of Aeronautics and Astronautics, Nanjing, 210016, China.
** Corresponding author.
E-mail addresses: liuyp@nuaa.edu.cn (Y. Liu), tangxiaobin@nuaa.edu.cn (X. Tang).

https://doi.org/10.1016/j.optcom.2024.130847
Received 13 March 2024; Received in revised form 17 June 2024; Accepted 5 July 2024
Available online 6 July 2024

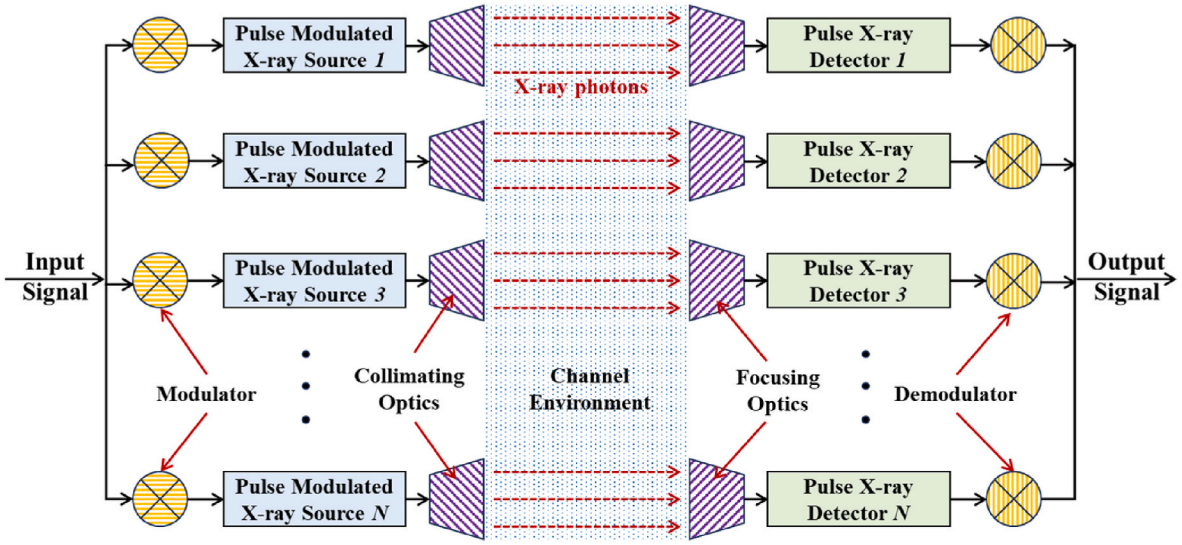

Fig. 1. Structure diagram of MIMO-XCOM.

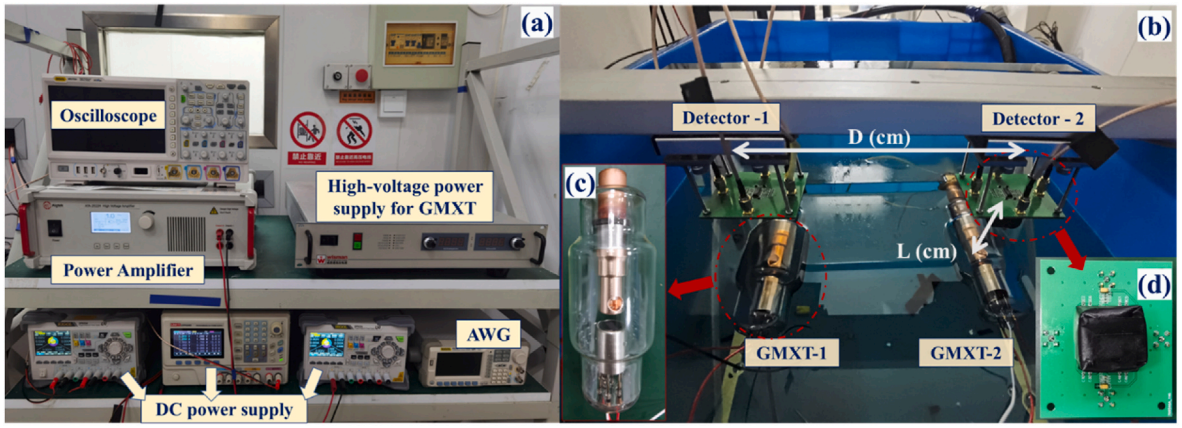

Fig. 2. (a) Photograph of the a two-receivers and two-transmitters array XCOM performance test system, (b) layout of the array detector, (c) GMXT, and (d) plastic scintillator coupled SiPM detector.

both the transmitter and the receiver need to be miniaturized, this array structure is bound to be affected by spatial correlation and signal crosstalk [19,20]. Therefore, it is essential to investigate the factors affecting the performance of array XCOM systems.

In this study, we analyzed the feasibility of array XCOM by constructing an array system using two GMXTs as transmitters and two plastic scintillators coupled with SiPMs as receivers. The relationship between the system's BER and the anode voltage, filament current, and array dimensions was analyzed, respectively. We clarified the relationship between array size and the correlation coefficient theoretically and demonstrated the impact of the array correlation coefficient on communication performance experimentally. We achieved a 3.6 Mbps communication rate while maintaining BER below the forward error correction (FEC) threshold.

2. Design of the array XCOM system

2.1. Experimental setup

The experimental setup diagram of the MIMO system is shown in Fig. 2. The grid-controlled modulated X-ray tube is well known for its mature process and affordable price. It was used as a transmitter in this experiment. Plastic scintillators have high transparency, short decay time, and high optical output, which offer the possibility of high-frequency X-ray detection. Thus, the plastic scintillator detector coupled with SiPM was selected as the receiver. On-off keying (OOK) modulation was employed in this experiment. A pseudorandom sequence was generated by an arbitrary waveform generator. The generated pulse voltage signal was amplified by a power amplifier and loaded on the grid of a GMXT, which generated produced pulse X-rays by bombarding the anode target with the electron beam. The on/off of X-rays can be controlled by switching the grid voltage. When the signal is "0", the grid voltage is −65 V, cutting off the electron beam completely and preventing the emission of X-rays. when the signal is "1", the grid voltage is 0 V, and the electron beam passes through the grid to bombard the anode target, generating X-rays. The energy and flux of X-ray photons are controlled by the anode voltage and filament current, respectively. The practical application scenario of XCOM is the low-density upper atmosphere and vacuum atmosphere, which is equivalent to the attenuation of long-distance transmission X-ray through the high-density lower atmosphere in the laboratory [21]. After passing through the air channel, the X-rays were detected by a plastic scintillator detector, and the resulting electrical pulse signal was recorded by a digital oscilloscope before being demodulated via threshold judgment and analyzed offline.

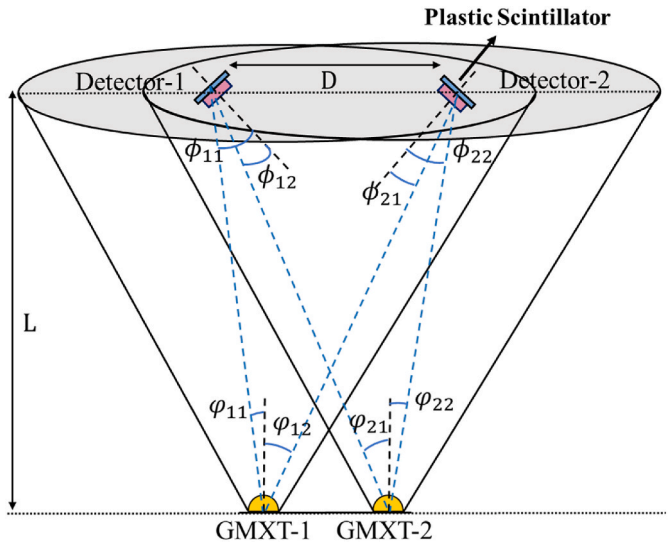

Fig. 3. Structure of a two-receivers and two-transmitters array XCOM system.

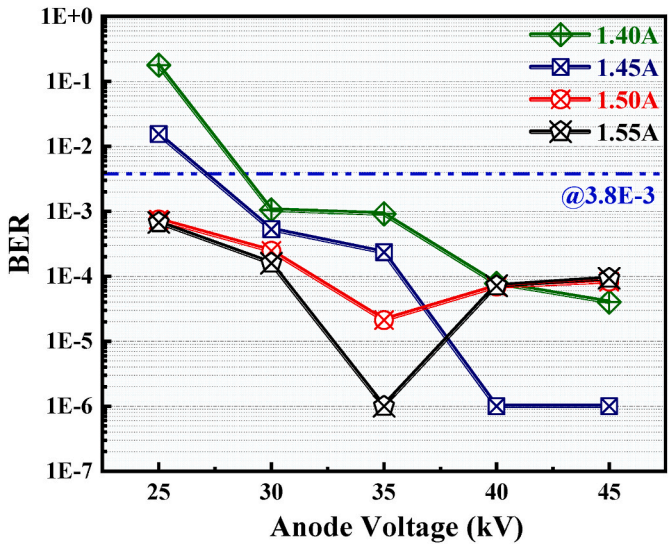

Fig. 4. BER versus filament currents and anode voltages.

2.2. The spatial correlation coefficient of arrays

Currently, XCOM primarily adopts intensity modulation to load information. Signal demodulation is accomplished at the receiver by detecting the radiation intensity information. The cross talk between different links is bound to exist in a system with multiple transmitters and receivers. We used the spatial correlation coefficient to characterize the ability of different receivers to transmit signals in parallel. The structure of a two-receivers and two-transmitters array XCOM system is shown in Fig. 3. The channel gain h is defined as the ratio of the received power P_r to the transmitted power P_t.

$$h = \frac{P_r}{P_t}, \tag{1}$$

For a system with multiple transmitters and multiple receivers, the channel matrix H can be expressed as

$$P_r = H * P_t, \tag{2}$$

where H is the channel transmission matrix, and h_{ij} represents the link gain received by the i-th receiver to the j-th transmitter.

$$H = \begin{vmatrix} h_{11} & h_{12} & \cdots & h_{1m} \\ h_{21} & h_{22} & \cdots & h_{2m} \\ \vdots & \vdots & h_{ij} & \vdots \\ h_{n1} & h_{n2} & \cdots & h_{nm} \end{vmatrix}, \tag{3}$$

where h_{ij} can be written as [22]

$$h_{ij} = \frac{1}{2\pi \int_0^{\frac{\theta_1}{2}} R_0(\phi)\sin(\phi)d\phi} \frac{A_s \cos(\varphi_{ij})}{d_{ij}^2} \eta_s R_0(\phi_{ij}), \tag{4}$$

where A_s is the detector area, $\theta_{1/2}$ is the maximum beam half angle, d_{ij} is the distance between the transmitter and receiver, η_s is the link attenuation coefficient, φ is the angle between the detector and the X-ray source normal, ϕ is the phase angle of the detector located at the X-ray source normal, and $R_0(\phi)$ is the power spectrum distribution.

The intensity of the X-rays produced by GMXT is uneven because of the structural design and packaging method. The non-uniformity of X-ray intensity distribution caused by the "heel effect" results in a large error when the conventional Lambert emission model is used to construct the emission pattern of GMXT. Given that the intensity of the X-rays emitted by the reflective X-ray tube shows a cosine distribution, the Gaussian function is used to fit the relative intensity function. The maximum beam half-angle is set to $\pi/13$. $R_0(\phi)$ can be modified as [22]

$$R_0(\varphi) = r_0 + \left[\frac{c_0}{a_0 \bullet (\pi/2)^{1/2}}\right] exp\left[-2\left(\frac{\varphi - \varphi_0}{a_0}\right)\right], \tag{5}$$

where

$c_0 = 17.347,\ \varphi_0 = -3.303^\circ,\ a_0 = 14.355,\ r_0 = 0.0505.$

The spatial correlation coefficient ρ_{ij}^t of the array system is defined as

$$\rho_{ij}^t = \frac{h_i h_j}{\|h_i\|\|h_j\|} = \frac{\sum_{k=1}^{2} h_{ki}h_{kj}}{\sqrt{\sum_{k=1}^{2} h_{ki}^2}\sqrt{\sum_{k=1}^{2} h_{kj}^2}}. \tag{6}$$

For an array of two transmitters and two receivers, ρ_{12}^t is given by

$$\rho_{12}^t = \frac{h_{11}h_{12} + h_{21}h_{22}}{\sqrt{h_{11}^2 + h_{21}^2} \times \sqrt{h_{12}^2 + h_{22}^2}}, \tag{7}$$

The system is left right symmetric. Thus,

$$h_{11} = h_{22},\ h_{12} = h_{21}, \tag{8}$$

The spatial correlation coefficient is expressed as follows by rectifying the above equation

$$\rho_{12}^t = \frac{2h_{11}h_{12}}{h_{11}^2 + h_{21}^2} = \frac{2\frac{1}{d_{11}^2 d_{12}^2} R_0(\varphi_{11})R_0(\varphi_{12})cos(\phi_{11})cos(\phi_{12})}{\frac{1}{d_{11}^4} R_0^2(\varphi_{11})cos^2(\phi_{11}) + \frac{1}{d_{12}^4} R_0^2(\varphi_{12})cos^2(\phi_{12})}. \tag{9}$$

3. Results and discussion

3.1. BER versus filament current and anode voltage

The electrical parameters of the GMXT directly affect the performance of the transmitter, so we first discuss its impact on communication performance. The transceivers of the array system are 10 cm apart, whereas the detectors are 5 cm apart. The communication rate is 1.8 Mbps, and the FEC threshold is 3.8E-3. We tested the performance of the array system under different anode voltages and filament currents, and the results are shown in Fig. 4. As the anode voltage increases, the energy of the X-ray photons increases. The BER of the two GMXT systems

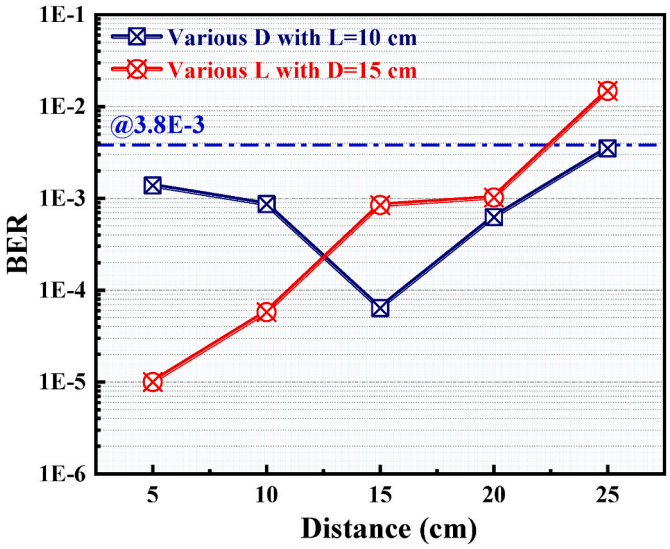

Fig. 5. BER versus geometric dimensions (The red line represents the performance of the array system at different GMXT distances with $D = 15$ cm; the dark blue line represents the performance of the array system at different detector distances, with $L = 10$ cm).

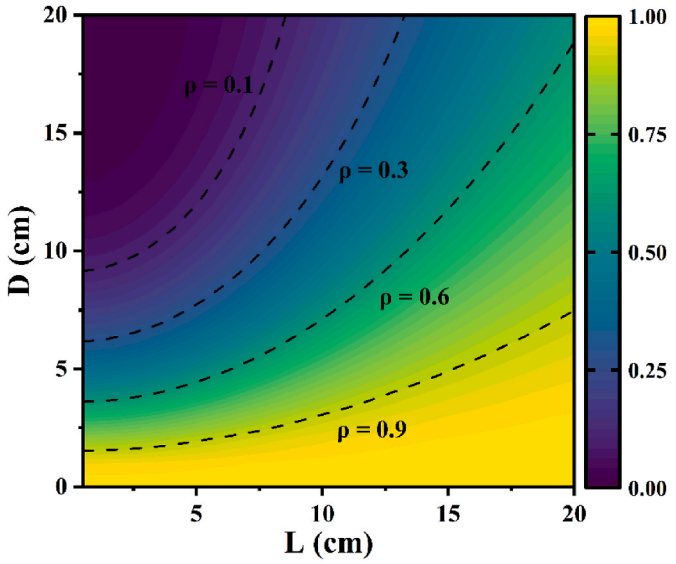

Fig. 6. Simulation result of spatial correlation coefficients ρ for different geometric dimensions base on Matlab (L is the distance from the GMXT to the detector, and D is the distance between the two detectors.).

shows a downward trend when the filament current is 1.40 A and 1.45 A, while the system BER decreases first and then increases when the filament current is 1.50 and 1.55 A. For the GMXT, the filament current determines the flux of the X-ray photons, and the anode voltage determines the energy of the X-rays. The two together determine the intensity distribution of the X-ray photons in space. As the intensity of the X-rays increases, the pulse amplitude of the detector gradually increases, and the threshold judgment becomes more accurate, so the BER will decrease. However, as the intensity increases, the detector is increasingly interfered by signals from different receivers. The detector simultaneously detects X-rays from multiple transmitters and superimposes them on the output signal waveform, causing some "0" signals to be mistakenly understood as "1" signals, resulting in an increase in the system BER. The source of the final system BER change is the competitive relationship between the two. At the same time, we noticed that at anode voltages, such as 35 kV, the system's BER changes significantly with the change in filament current. This is because the plastic scintillator detector is more sensitive to X-ray flux. When the filament current is 1.40 A, the anode voltage increases from 30 kV to 40 kV, and the detector pulse amplitude only increases by about 10 mV, and the pulse amplitude after the increase is about 50 mV. When the tube voltage is 40 kV, the filament current increases from 1.40 A to 1.50 A, and the detector output pulse amplitude increases by about 150 mV, and the pulse amplitude after the increase is about 200 mV. Because in the actual communication process, the plastic scintillator pulse amplitude has a certain random jitter effect (the jitter amplitude is generally around 15 mV), when the pulse amplitude is low, this jitter poses a great challenge to the accuracy of the threshold judgment. As the pulse amplitude increases, the impact of this effect can be eliminated by setting a higher threshold voltage.

3.2. BER versus geometric dimension

The dimension of the array is one of the important parameters of the array structure, and its impact on communication performance is crucial. Fig. 5 shows the performance of the array system with different geometric dimensions. Here D is the distance between the detectors, and L is the distance between the GMXT and detector. The array system only has two GMXTs and detectors. Thus, changing the distance between them independently has the same spatial effect. In this experiment, the anode voltage is 40 kV, the filament current is 1.45 A, and the array's communication rate is 1.8 Mbps. The distance between the GMXT and detector is 10 cm. When the detectors are close together, the detectors will receive signals from different GMXTs simultaneously, affecting the signal determination. As D increases, the BER improves. However, when D is larger than 15 cm, the detector gradually deviates from the field of view of the transmitters, the number of received photons decreases, and the BER starts to increase again gradually. As the distance L increases, the number of X-ray photons received by the detector decreases, the generated pulse waveform decreases, and the amplitude of the output signal strength weakens, thereby increasing BER.

3.3. BER versus spatial correlation

Owing to the OOK modulation used in this experiment, we determine whether the signal is "0" or "1" by the intensity change of the X-rays. The ideal situation for an array system is that the receiver only receives the signal from its corresponding transmitter, and the signals from different transmitters do not interfere with each other in space. However, the X-ray signals from various transmitters are superimposed inevitably in space. Moreover, the XCOM system channel is a line-of-sight (LOS) link, and the X-rays emitted by GMXT have a divergence angle, exacerbating the array system's spatial correlation. On the basis of the analysis in Section 2.2, we used the spatial correlation coefficient to describe the system's ability to transmit signals independently and parallelly. The correlation coefficients ρ of the array system with different geometrical dimensions were simulated by MATLAB. The results are shown in Fig. 6. When D is certain, the differentiation of the X-ray signals received from different transmitters gradually decreases as L increases, and the spatial correlation coefficient increases. When L is certain, the influence of the transmitter on the noncorresponding receiver gradually decreases as D increases, and the spatial correlation coefficient decreases.

We change the spatial correlation coefficient of the system by adjusting the array size. Although both XCOM and visible light communication (VLC) have a high correlation coefficient [19,23], VLC is frequently affected by photon scattering in different paths [24], whereas this effect is insignificant in XCOM due to X-rays' high penetration. Therefore, even if the correlation coefficients of those two types of communications are the same, the impact of the correlation coefficients on communication performance is different. Since the transmitters must be miniaturized in actual deployment, the situation of $\rho = 0$ is difficult to

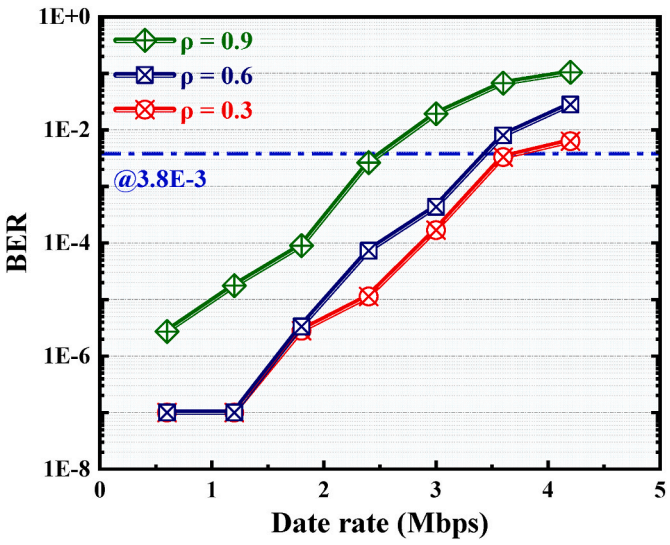

Fig. 7. Experimental result of BER versus spatial correlation coefficient.

achieve. To illustrate the effect of different spatial correlation coefficients on system performance, a test was done under various spatial correlation coefficients of ρ = 0.3, 0.6, and 0.9, respectively, and the experimental results are shown in Fig. 7. In this experiment, each BER point tested about 6 M bits. When there is no error bit, it is recorded as 1E-7 in the logarithmic coordinate graph, as shown in Figs. 7 and 8. As the correlation coefficient increases, the overall performance of the system decreases. At the same data rate, when ρ = 0.3 the system's BER is 1–2 orders of magnitude lower than that of ρ = 0.9. Similarly, at the BER of 3.8E-3, when ρ = 0.3, the system's data rate increased by approximately 1Mbps compared to ρ = 0.9.

3.4. BER versus data rate

The maximum communication data rate is an important criterion for evaluating a communication system's performance. Owing to the need for miniaturization design of multiple transceivers in actual communication processes, there is inevitably a certain correlation in the system. Taking a medium correlation coefficient of $\rho \approx 0.5$ with L = 12.5 cm, and D = 10 cm as an example, we tested the maximum data rate when the anode voltage was set to 50 kV and filament current was 1.50 A. The results are shown in Fig. 8. The performance of the experimental system in SISO mode and MIMO mode are shown as black lines and red lines respectively. Array system can bring a gain of 1.6 Mbps to the XCOM system. Compared with previous works of Refs. [8], [12], [22], and [25], the array system is able to effectively increase the data rate. Under the condition that the bit error rate is 3.8E-3, the data rate of the developed array system is increased by 1.7 Mbps. Even when the data rates are all about 1.2 Mbps, the BER of the array system is significantly low. This result that despite the presence of correlation interference, the developed MIMO-XCOM system still has good performance.

The eye diagram is one of the most effective means to detect signal integrity. An eye diagram test on the scintillator output signal was performed at 1.2 and 3.6 Mbps, as shown in Fig. 8(b) and (c), respectively. The eye diagrams of the two detectors are relatively similar at the same data rate, so we only show one of them here. The interference between adjacent bits at a low rate is minimal. Thus, the eye diagram features are relatively intact. The interference between two adjacent bits becomes obvious when the data rate reaches up to 3.6 Mbps. Moreover, the high level has obvious fluctuation, and the low level does not return suitably to the "0" position. Thus, demodulating the signal based on threshold judgment becomes difficult. Finally, the communication rate of the array system reaches 3.6 Mbps with an FEC threshold of less than 3.8E-3.

4. Conclusion

In this work, we used a MIMO approach in constructing a two-transmitter, two-detector array XCOM to improve the system's performance. The effects of various working parameters and array dimensions on the BER of the system were investigated. The spatial correlation coefficient of the array system was calculated theoretically. Compared with the system's BER when ρ = 0.3, that when ρ = 0.9 increases by 1–2 orders of magnitude and the corresponding maximum communication data rate decreases by 1 Mbps. The array system achieves a communication data rate of 3.6 Mbps in a 12.5 cm laboratory air channel with

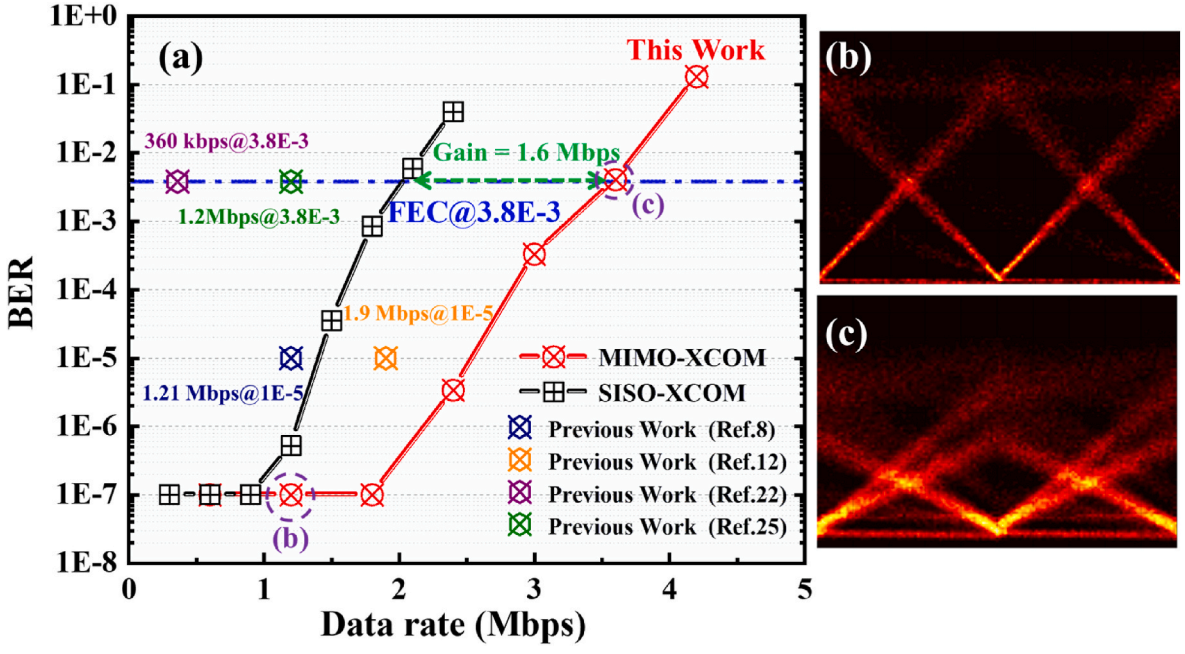

Fig. 8. (a)BER versus data rata of XOCM, (b) eye diagram at data rata is 1.2 Mbps and (c) eye diagram at data rata is 3.6 Mbps

spatial correlation coefficient at 0.5 and BER below the FEC threshold of 3.8E-3. Compared with previous works, under the same BER, the data rate of the array system is increased by 1.7 Mbps. The array system still has advantages in BER even at the same data rate. To the best of our knowledge, this is the first experiment to build a multi-input multi-output XCOM system. This study proposes a new idea to increase data rate and lays the foundation for the design of a MIMO array XCOM system.

Funding

Project supported by the National Natural Science Foundation of China (Grant No. 12375256), the Fundamental Research Funds for the Central Universities (Grant No. NT2023012), and the Foundation of Graduate Innovation Center in NUAA (Grant No. xcxjh20220609).

CRediT authorship contribution statement

Hao Chi: Writing – review & editing, Software, Data curation. **Yunpeng Liu:** Writing – review & editing, Validation, Supervision, Funding acquisition. **Junxu Mu:** Writing – review & editing, Supervision, Investigation. **Feixu Xiong:** Writing – review & editing, Supervision, Project administration. **Xiaobin Tang:** Writing – review & editing, Funding acquisition, Formal analysis.

Declaration of competing interest

The authors declare that they have no known competing financial interests or personal relationships that could have appeared to influence the work reported in this paper.

Data availability

Data will be made available on request.

References

[1] P.J. Winzer, Would scaling to extreme ultraviolet or soft X-ray communications resolve the capacity crunch, J. Lightwave Technol. 36 (24) (2018) 5786–5793, https://doi.org/10.1109/JLT.2018.2877575.
[2] B. Zhao, C. Wu, L. Sheng, Y. Liu, Next generation of space wireless communication technology based on X-ray, Acta Phys. Sin. 42 (7) (2013) 801–804, https://doi.org/10.3788/gzxb20134207.0801.
[3] Y. Li, T. Su, L. Sheng, et al., X-ray transmittance characteristics and potential communication in re-enter plasma sheath, Optik 197 (2019) 162917, https://doi.org/10.1016/j.ijleo.2019.06.017.
[4] H. Li, X. Tang, S. Hang, et al., Potential application of X-ray communication through a plasma sheath encountered during spacecraft reentry into earth's atmosphere, J. Appl. Phys. 121 (12) (2017) 123101, https://doi.org/10.1063/1.4978758. American Institute of Physics.
[5] Z. Feng, Y. Liu, X. Tang, et al., Optimization and testing of groove-shaped grid-controlled modulated X-ray tube for X-ray communication, Nucl. Instrum. Methods Phys. Res., Sect. A 1026 (2022) 166218, https://doi.org/10.1016/j.nima.2021.166218.
[6] H. Xuan, Y. Liu, P. Qiang, et al., Light-controlled pulsed x-ray tube with photocathode, Chin. Phys. B 30 (11) (2021) 118502, https://doi.org/10.1088/1674-1056/abff1e.
[7] Y. Liu, H. Xuan, L. Sheng, et al., X-ray communication experiment using photocathode x-ray tube, Proc. SPIE-Int. Soc. Opt. Eng. 11763 (2021), https://doi.org/10.1117/12.2587619.
[8] J. Mu, X. Tang, Y. Liu, et al., Design and performance test of pulse X-ray receiver based on LYSO-SiPM for X-ray communication, J. Lightwave Technol. 40 (13) (2022) 4217–4223, https://doi.org/10.1109/JLT.2022.3162344.
[9] J. Yin, Y. Liu, F. Xiong, et al., Avalanche photodiode detection system enables X-ray communication up to 10 Mbps, Methods Phys. Res., Sect. A 1049 (2023) 168048, https://doi.org/10.1016/j.nima.2023.168048.
[10] Y. Wang, Y. Liu, X. Tang, et al., Collimating/focusing optical system designed for hard X-ray communication, Nucl. Instrum. Methods Phys. Res., Sect. A 1016 (2021) 165776, https://doi.org/10.1016/J.NIMA.2021.165776.
[11] T. Su, L. Tang, B. Zhao, et al., An X-ray frequency modulation method and its application in X-ray communication, Optik 199 (2019) 163263, https://doi.org/10.1016/j.ijleo.2019.163263.
[12] Y. Li, T. Su, L. Sheng, et al., Simulation and experiment of X-ray communication in re-entry dusty plasma region, Mod. Phys. Lett. B 34 (4) (2020) 2050057, https://doi.org/10.1142/S0217984920500578.
[13] G. Timofeev, N. Potrakhov, A. Gryaznov, Data transmission in the X-ray emission frequency range of electromagnetic radiation, J. Russian Univer. Radioelectron. 24 (2) (2021) 6–17, https://doi.org/10.32603/1993-8985-2021-24-2-6-17.
[14] T. Reinecke, S. Kenyon, K. Gendreau, et al., Characterization of a modulated X-ray source for ion mobility spectrometry, Anal. Chem. 94 (35) (2022) 12008–12015, https://doi.org/10.1021/acs.analchem.2c00729.
[15] G. Timofeev, N. Potrakhov, A. Nechaev, Experimental research of the x-ray communication system, AIP Conf. Proc. AIP Pub. LLC 2089 (1) (2019) 020020, https://doi.org/10.1063/1.5095749.
[16] M.D. Renzo, H. Haas, P.M. Grant, Spatial modulation for multiple-antenna wireless systems: a survey, IEEE Commun. Mag. 49 (12) (2021) 182–191, https://doi.org/10.1109/MCOM.2011.6094024.
[17] W. Yuan, et al., Theoretical and simulation analysis of a novel multiple-input multiple-output scheme over multimode fiber links with dual restricted launch techniques, Opt. Eng. 51 (6) (2012) 065002, https://doi.org/10.1117/1.OE.51.6.065002.
[18] X. Guo, T. Chu, J. Xia, Superposed three-dimensional 64QAM constellation design for MIMO-OFDM visible light communication systems, Opt Express 31 (22) (2023) 35850–35863, https://doi.org/10.1364/OE.502169.
[19] D. Zheng, H. Zhang, J. Song, et al., Spatial multiplexing MIMO visible light communications with densely distributed LEDs and PDs, IEEE Photon. J. 12 (5) (2020) 7905807, https://doi.org/10.1109/JPHOT.2020.3029185.
[20] V. Dixit, A. Kumar, Error performance of an L-PPM modulated ADR-based MIMO-VLC system with and without channel estimation error, Appl. Opt. 62 (10) (2023) 2501–2509, https://doi.org/10.1364/AO.478994.
[21] Y. Li, T. Su, B. Zhao, et al., Bit error rate analysis of the spatial X-ray communication system, Infrared Laser Eng. 47 (6) (2018) 622001, https://doi.org/10.3788/irla201847.0622001.
[22] W. Chen, Y. Liu, X. Tang, et al., Experimental evaluation of an OFDM-PWM-based X-ray communication system, Opt Express 29 (3) (2021) 3596–3608, https://doi.org/10.1364/OE.415291.
[23] O. Alamu, Thomas O. Olwal, K. Djouani, et al., Cooperative visible light communications: an overview and outlook, Opt. Switch. Netw. 52 (2024) 100772, https://doi.org/10.1016/j.osn.2024.100772.
[24] M. Oliveira, L. Vieira, F. Guiomar, et al., Experimental assessment of the performance of cooperative links in visible light communications, Opt Commun. 524 (2022) 128771, https://doi.org/10.1016/j.optcom.2022.128771.
[25] F. Xiong, Y. Liu, J. Yin, et al., SIPAM-4 scheme improves bit error rate performance in MISO X-ray communication system, Optik 287 (2023) 171059, https://doi.org/10.1016/j.ijleo.2023.171059.